AGU PUBLICATIONS

Geophysical Research Letters

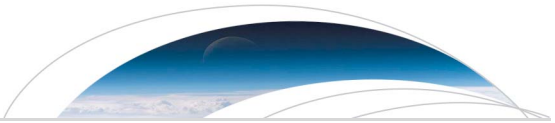

RESEARCH LETTER
10.1002/2017GL075434

Key Points:
- Snow and ice thickness and northern extent of multiyear ice were observed in April 2017 with unique in situ measurements
- Modal, total ice thickness ranged between 1.8 and 3.2 m, little different from 2011 and 2014, but 0.75 m thinner than in 2004, and consistent with thinning rates over 2000–2012
- Mean and modal snow thicknesses varied strongly between 0.3 to 0.47 m and 0.1 to 0.5 m, respectively, in close agreement with climatology

Supporting Information:
- Supporting Information S1

Correspondence to:
C. Haas,
chaas@awi.de

Citation:
Haas, C., Beckers, J., King, J., Silis, A., Stroeve, J., Wilkinson, J., Notenboom, B., Schweiger, A., & Hendricks, S. (2017). Ice and snow thickness variability and change in the high Arctic Ocean observed by in situ measurements. *Geophysical Research Letters*, *44*, 10,462–10,469. https://doi.org/10.1002/2017GL075434

Received 24 AUG 2017
Accepted 4 OCT 2017
Accepted article online 9 OCT 2017
Published online 25 OCT 2017

Ice and Snow Thickness Variability and Change in the High Arctic Ocean Observed by In Situ Measurements

Christian Haas[1,2], Justin Beckers[2,3], Josh King[4], Arvids Silis[4], Julienne Stroeve[5], Jeremy Wilkinson[6], Bernice Notenboom[7], Axel Schweiger[8], and Stefan Hendricks[1]

[1]Alfred Wegener Institute of Polar and Marine Research, Bremerhaven, Germany, [2]Department of Earth and Space Science and Engineering, York University, Toronto, Ontario, Canada, [3]Department of Earth and Atmospheric Sciences, University of Alberta, Edmonton, Alberta, Canada, [4]Climate Research Division, Environment and Climate Change Canada, Toronto, Ontario, Canada, [5]Centre for Polar Observation and Modeling, University College London, London, UK, [6]British Antarctic Survey, Cambridge, UK, [7]Fernie, British Columbia, Canada, [8]Polar Science Center, University of Washington, Seattle, Washington, USA

Abstract In April 2017, we collected unique, extensive in situ data of sea ice and snow thickness. At 10 sampling sites, located under a CryoSat-2 overpass, between Ellesmere Island and 87.1°N mean and modal total ice thicknesses ranged between 2 to 3.4 m and 1.8 to 2.9 m, respectively. Coincident snow thicknesses ranged between 0.3 to 0.47 m (mean) and 0.1 to 0.5 m (mode). The profile spanned the complete multiyear ice zone in the Lincoln Sea, into the first-year ice zone farther north. Complementary snow thickness measurements near the North Pole showed a mean thickness of 0.31 m. Compared with scarce measurements from other years, multiyear ice was up to 0.75 m thinner than in 2004, but not significantly different from 2011 and 2014. We found excellent agreement with a commonly used snow climatology and with published long-term ice thinning rates. There was reasonable agreement with CryoSat-2 thickness retrievals.

1. Introduction

Arctic sea ice extent is strongly decreasing (e.g., Meier et al., 2014), and there is clear evidence from in situ, airborne, and satellite observations that the ice is also thinning (e.g., Haas et al., 2008; Lindsay & Schweiger, 2015; Meier et al., 2014). These changes already affect the Arctic climate, ecosystem function, and the livelihood of people living in that region. Ice thickness observations are particularly important as they provide information about the deformation and redistribution of ice, which ultimately lead to the observed patterns of sea ice extent variability and change. However, there is still a sparsity of ice thickness observations, and comparability across different methods is often difficult, hindering the compilation of consistent data sets. There are programs that provide extensive airborne (e.g., Haas et al., 2010; Richter-Menge & Farrell, 2013) and satellite measurements (e.g., Kwok & Cunningham, 2015); however, these either only span short observational periods yet, or are subject to large retrieval uncertainties. Likewise, in situ measurements are scarce due to the harsh environment, logistical difficulties, and cost constraints, although they do provide the most accurate, targeted data so urgently required for calibration and validation of airborne and satellite observations. A common source of in situ sea ice thickness data are automatic drifting buoys; however, their observations are local and cannot account for the enormous spatial variability of snow and sea ice thickness (e.g., Perovich & Richter-Menge, 2015).

Here we present results from in situ measurements from the European Space Agency's (ESA) CryoSat-2 Validation Experiment (CryoVEx) 2017 campaign in April 2017, an effort to collect accurate, representative in situ snow and ice thickness data between Ellesmere Island and the North Pole (Figure 1). In order to assess the large concurrent local and regional variability of snow and ice thickness, we collected extensive high-resolution data at as many individual sampling sites as was possible within the available time and budget. These measurements give unique insights into the present state of sea ice in one of the most difficult to reach regions of the Arctic Ocean. To put these measurements in context, we compare them with similar but much more limited measurements carried out in the same region since 2004. Of particular importance is that our data show initial ice conditions at the beginning of the 2017 melt season (i.e., maximum ice thickness),

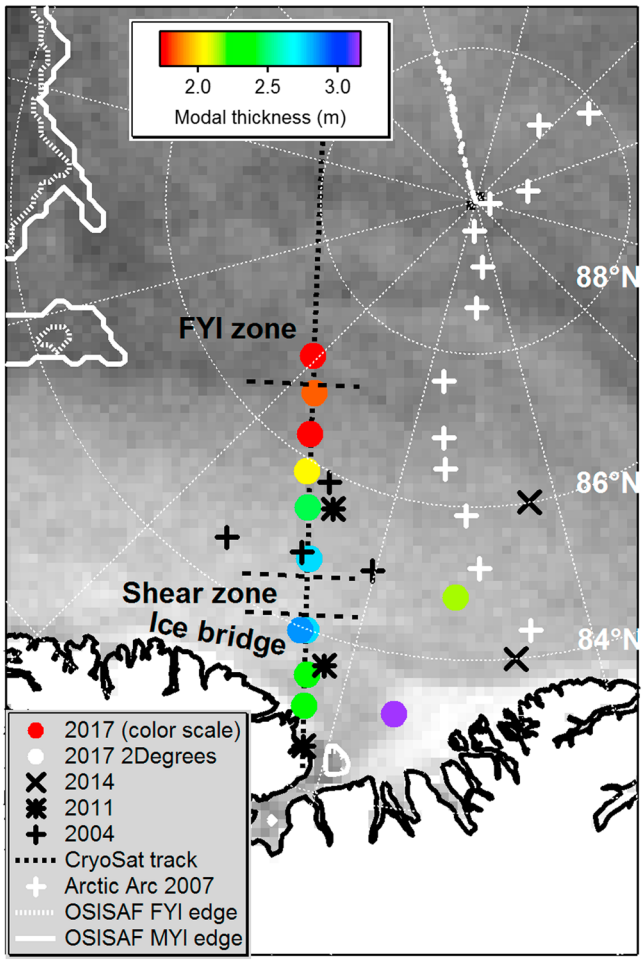

Figure 1. Map of CryoVEx 2017 sampling locations along CryoSat-2 orbit 37159 (black dotted line) and two sites in the northeast, color coded by modal total ice thickness. Small white dots show locations of the 2017 2Degrees Expedition snow measurements. Also shown are locations of previous ice (black symbols) and snow (white crosses) thickness measurements, OSISAF ice type boundaries (OSISAF classified first-year ice only in upper left corner), and our own ice regime boundaries based on visual observations and SAR imagery. Background shows uncalibrated radar backscatter from the ASCAT scatterometer (courtesy G. Spreen, University of Bremen) representative of ice conditions on 18 April 2017, the last day of sampling.

and thus support international efforts to predict seasonal sea ice development leading to the 2017 summer sea ice minimum (e.g., Lindsay et al., 2012; Stroeve et al., 2015). Sites were aligned along a CryoSat satellite track and collocated with CryoVEx and NASA Operation IceBridge (OIB) aircraft profiles to provide validation data and to facilitate extrapolation of in situ results to larger regions under the aircraft and satellite flight tracks.

A particular focus of our CryoVEx 2017 measurements was extensive snow thickness measurements collocated together with the ice thickness soundings. To date, in situ measurements are still the only means of accurate snow thickness observation (e.g., Gerland & Haas, 2011; King et al., 2015; Sturm et al., 2006). These are invaluable for the validation of airborne and satellite snow thickness retrievals (e.g., King et al., 2015) and for the evaluation of the Warren snow thickness climatology (Warren et al., 1999; henceforth W99) which is commonly used as the only data source to support airborne and satellite ice thickness retrievals (e.g., Kurtz & Farrell, 2011; Laxon et al., 2013).

2. Methods and Measurements

2.1. Study Region and Sampling Site Selection

All snow and ice thickness measurements were carried out over 6 days between 11 and 18 April, at 12 sampling sites located between Ellesmere Island and a latitude of 87.1°N, approximately 30 nautical miles apart (Figure 1, Table S1 in the supporting information). Ten sites were aligned along a main profile in northwesterly direction, coincident with CryoSat-2 (orbit 37159) and OIB overflights on 12 April. In addition, two sites toward the northeast were sampled on 17 April.

In general, the sea ice cover is a patchwork of apparently undeformed, level ice patches separated by hummocks, ridges, rubble fields, and open and refrozen leads (e.g., Haas, 2017). In the multiyear ice zone, where winter ice concentrations are consistently high, large level ice patches mostly represent ice of the same age that has undergone the same freezing and melting conditions. Over several years, melt pond formation creates a significant microtopography on and under the ice. The thickness of these level ice patches is a representative climate indicator, represented by the thickest mode of a thickness distribution (e.g., Haas et al., 2008; Renner et al., 2014). Furthermore, level ice strongly affects the responses of airborne and satellite radar instruments. Therefore, we aimed at preferentially sampling over several of such large level ice patches at each sampling site. We note that thick, deformed ice is included but underrepresented in our data set, leading to somewhat smaller estimates of mean ice thickness and complicating comparisons with other thickness observations.

All sampling sites were visited by ski-equipped DHC-6 Twin Otter aircraft operated out of the Canadian Forces Station Alert on the northern tip of Ellesmere Island (Figure 1). Landing an aircraft on unprepared sea ice is highly demanding and requires sea ice of sufficient thickness, smoothness, length, and direction with regard to the wind (Verall, 2000). Such conditions are typically offered by old first-year ice on refrozen leads. Here we additionally required the proximity of these landing sites to suitable level multiyear or old first-year ice patches to meet the scientific requirements stated above.

We complement our snow observations with snow thickness measurements carried out between 4 and 21 April 2017, during the Two Degrees (2Degrees) ski expedition in a region between 88°N, 150°E and the North Pole (Figure 1; Notenboom et al., 2017).

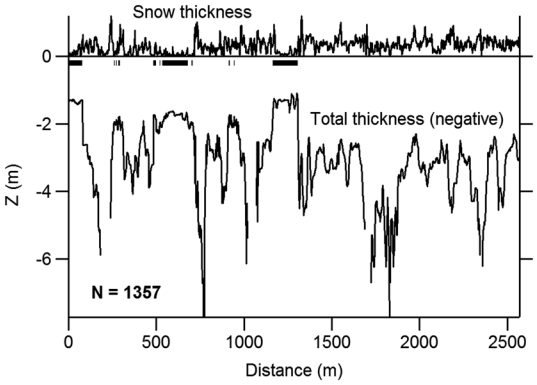

Figure 2. Typical data set of collocated snow and ice thickness. Ice thickness plotted with negative sign to illustrate approximate ice draft. Thick bars just below horizontal zero line show locations identified as thin first-year ice not used in analysis. Data from site 5.

2.2. Ice Thickness Measurements

Ice thickness measurements were performed by means of ground-based electromagnetic induction (EM) sounding, used for accurate and quick surveys of large regions (e.g., Haas et al., 1997; Haas et al., 2008; Renner et al., 2014). EM sounding is sensitive to the high electrical conductivity of seawater, but cannot distinguish between the highly resistive layers of snow and ice. Therefore, snow and ice are measured together and yield an estimate of total, that is, snow plus ice thickness. For better comparison with previous studies, here we decided to continue to use estimates of total thickness, instead of subtracting coincidentally measured snow thicknesses (Figure 2).

Instead of commonly used, long EM instruments, here we used a short Geonics EM31SH instrument for better versatility (http://geonics.com/html/em31-mk2.html). It has a coil spacing of only 2 m and operates with a signal frequency of 9.8 kHz. The instrument was mounted onto a small toboggan and operated in horizontal dipole mode (Figure S1) and was dragged while walking along the profiles. Data were acquired with a sampling frequency of 1 Hz and were georeferenced by Global Positioning System (GPS) positioning. The GPS data were used to resample the EM measurements to an equidistant point spacing of 5 m, to correct for variable walking speed and stops. They will later also be used to carry out ice drift correction and to resample the EM measurements to the exact locations of the snow thickness measurements (see below). In total, 7,348 measurements were carried out, amounting to a total profile length of 36,735 m ranging from 1,760 m to 4,995 m at each site.

At each site, two or three drill hole measurements were carried out at the location of EM measurements to confirm the proper calibration of the instrument (see Figure S2). The data show that even with the shorter instrument, the accuracy of the EM measurements is ±0.1 m over level ice up to 4 m thick. EM measurements over rough, deformed ice are less accurate, and maximum ridge thicknesses can be underestimated by as much as 50% (Haas & Jochmann, 2003).

2.3. Snow Thickness Measurements

Snow thickness measurements were carried out with Snow-Hydro Magnaprobes (http://www.snowhydro.com) equipped with a data logger and GPS. They have an expected precision of 3 mm (Sturm et al., 2006). Measurements were performed with a constant spacing of two to four steps, corresponding to a distance of 1–3 m, depending on the operator. They were carried out along the same profiles as the EM ice thickness measurements, following the tracks in the snow (Figure 2). However, due to the slower progress of snow thickness measurements, profiles were shorter than the ice thickness profiles. For this study we computed summary statistics for the complete, individual snow and ice thickness data sets. Before doing so, the ice thickness data were used to identify and remove ice and snow thickness data over thin, refrozen leads at the landing sites to avoid biases due to thin young ice (Figure 2). In total, 10,574 snow thickness measurements were carried out over thick ice, ranging from 113 to 2,417 at each site.

At each site one to several snow pits were sampled on old ice. Here we used vertical profiles of snow salinity to help classify sampling sites into first-year or multiyear ice.

During the 2Degrees ski expedition, only snow thicknesses were measured, using graded ski poles with a precision of 5 mm. At each of a total of 47 sites approximately 5 to 10 km apart, 10 measurements with a point spacing of approximately 4 m were carried out (Notenboom et al., 2017). As this approach is quite different from the approach of extensive measurements at fewer sites described above, here we averaged all measurements within each degree of latitude (n = 290 between 88 and 89°N and n = 180 between 89 and 90°N) to obtain more representative results.

3. Results

3.1. Ice Types

Figure 1 shows the boundaries between major ice regimes sampled in April 2017. Ice regimes were identified based on visual observations during the sampling flights and on synthetic aperture radar (SAR) imagery.

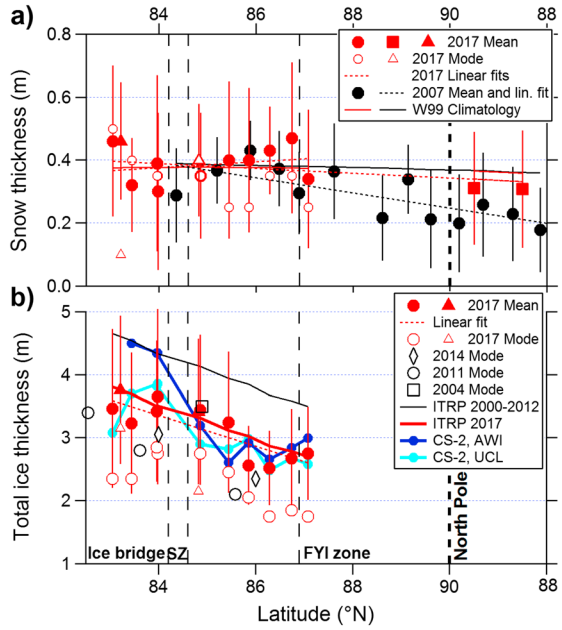

Figure 3. Present and past observed (a) snow and (b) ice thicknesses versus latitude, from Ellesmere Island (left) across the North Pole to the eastern Arctic (cf. Figure 1 for locations). Red symbols show measurements in April 2017, black from previous years. Closed symbols show mean thicknesses (with error bars indicating ±1 standard deviation), open symbols show modes. Red circles show mean thicknesses along the main transect in 2017, triangles show thicknesses at the two sites closer to Greenland (cf. Figure 1). Dotted lines show linear fits to mean thicknesses. In Figure 3a, solid red and black lines show W99 climatological snow thickness for the 2017 and 2007 data, respectively. In Figure 3b, solid black and red lines show ITRP climatological mean ice thicknesses for the 2000–2012 reference period and predicted for 2017. Blue symbols show thicknesses retrieved from the Alfred Wegener Institute (AWI) and University College London (UCL) CryoSat-2 products. Thin vertical stippled lines show ice regimes identified in Figure 1.

During this season there was an immobile fast ice bridge along the coasts of Ellesmere Island and Greenland. This region was separated from the mobile multiyear and second year ice to the north by a prominent shear zone. The shear zone consisted of many deformed floes and open leads and as such landing was not possible. While there were increasing fractions of first-year ice in the region of the northern three sites, the northernmost site was clearly located in the predominantly first-year ice zone, interspersed with few small chunks of heavily hummocked multiyear ice.

The classification of ice types is supported by the observed snow salinities. At most sites these ranged between 0 and 0.4 ppt, but at the northernmost site were as high as 11.3 ppt, supporting attribution of this site as first-year ice. With this distribution of sampling sites, the goal of traversing the complete multiyear ice zone in the region was successfully met.

3.2. Ice Thickness

Results of the ice thickness measurements are presented in Figures 1, 3b, and S3 and Table S1, showing the transition from the thickest, oldest ice in the south to the first-year ice in the north. Mean, total ice thicknesses ranged between 2.5 and 3.8 m, excluding refrozen leads, with standard deviations in the range of 0.6 to 1.2 m. The thickest ice was found in the vicinity of the shear zone and at the site nearest to Greenland. The thinnest ice was located farthest to the north, representing second- and old first-year ice. As a first-order approximation, a linear fit to the data along the CryoSat-2 orbit yielded a meridional relationship of

$$\text{Ice thickness (m)} = 23.9\ \text{m} - 0.24\ \text{m degree}^{-1} \times \text{Latitude (degrees)}$$

with a correlation coefficient of $r = 0.82$ (Figure 3b). The mean thickness along that transect was 3.1 m.

Modal, total thicknesses ranged between 1.8 and 3.2 m, including 0.25 to 0.4 m of snow (see below). At all three northernmost sites it was only 1.8 to 1.9 m, with little difference between second- and first-year ice.

3.3. Snow Thickness

In contrast to the ice, no clear spatial snow thickness gradients were observed between Ellesmere Island and 87.1°N. Mean snow thickness was 0.39 ± 0.06 m, and mean modal thickness was 0.34 ± 0.08 m. Mean snow thickness east of the North Pole observed by the 2Degrees expedition was 0.31 ± 0.00 m, that is, somewhat thinner than along our main transect (Figure 3a). There was large variability from site to site. Mean and modal snow thicknesses ranged between 0.3 to 0.47 m, and 0.1 to 0.5 m, respectively (Figure 3a and Table S1). On average, the snow thickness standard deviation at each site was 58% of the mean thickness. Even at sites with thick snow on average, bare shallow hummocks without significant snow cover did frequently occur.

4. Discussion

How did the observed ice and snow thicknesses compare with previous years? There are only few comparable in situ data available, and below we compare our 2017 measurements with those, with commonly used climatologies, and with CryoSat-2 thickness retrievals.

Figure 3b includes results of EM ice thickness measurements similar to those described here. They were carried out during the GreenICE 2004 (Haas et al., 2006) and CryoVEx 2011 (Willatt & Haas, 2011; Kwok & Haas, 2015) and 2014 (Beckers et al., 2015) field campaigns. While sampling locations in 2004 and 2011 were approximately coincident with our 2017 survey, the CryoVEx 2014 measurements were

farther to the east (Figure 1 and Table S1). As profiles in 2004–2014 were much shorter and mostly included level ice only, we pooled all measurements in each year and only show modal thicknesses (Figure 3b). It can be seen that modal thicknesses observed in 2011 and 2014 show similar northward gradients, and fall within the range of modal thicknesses as in 2017. Thus, results indicate that there was little thinning of level ice in recent years. However, modal thickness in 2004 was 3.5 m, 0.75 m thicker than in the same region in 2017.

Figure 3b also shows a comparison of our results with an ice thickness climatology compiled by Lindsay and Schweiger (2015), which is based on a range of different observations collected between 2000 and 2012. The figure shows the result of their Ice Thickness Regression Procedure (ITPR) applied to our main northwesterly transect. Results represent mean ice thicknesses without snow, and we have added our observed mean snow thickness of 0.39 m to the ITPR results to be comparable with our observations of mean total thickness. The mean total thickness of the 2000–2012 ITPR results is 4.1 m, that is, 1.0 m thicker than our observations in 2017. This thinning rate is of similar magnitude as the 0.75 m of thinning observed for modal thicknesses since 2004 discussed above, although mean and modal thicknesses depend on different thermodynamic and dynamic forcing. The figure also includes temporally extrapolated ITPR results for 2017 based on a trend of -0.58 ± 0.07 m decade^{-1} between 2000 and 2012 derived by Lindsay and Schweiger (2015). There is good agreement between the latitudinal gradients, and the extrapolated ITPR mean total thickness of 3.2 m is only 0.1 m thicker than observed here. This suggests that on average, sea ice thinning in this region has continued at rates similar as observed between 2000 and 2012.

Finally, Figure 3b also shows mean monthly CryoSat-2 ice thicknesses at the sampling locations extracted from the near-real-time, gridded products of Alfred Wegener Institute (AWI) (Hendricks et al., 2016) and University College London (UCL) (Tilling et al., 2016). Like above, 0.39 m was added to both products to account for mean snow thickness. Both CryoSat data sets represent the general gradients quite well, from the thick multiyear ice to thin first-year ice. Mean thickness of both products is 3.48 m (UCL) and 3.77 m (AWI), that is, 0.38 m and 0.67 m thicker than our observations, respectively. While both CryoSat data sets agree well with each other over the thinner ice to the north, the AWI data are 0.8 m thicker than the UCL data over the thickest ice. Differences are due to different processing algorithms and may be sensitive to different ice surface roughness. For example, the AWI product shows very thick ice in the region of prominent shear ridges in the region of the ice bridge (Figure S4). These differences demonstrate the difficulties of validating CryoSat data with limited in situ measurements. Further analysis is beyond the scope of this study.

Figure 3a compares the observed snow thicknesses with the W99 climatology for April and with in situ measurements carried out by the ArcticArc ski expedition in 2007 (Gerland & Haas, 2011). Along our main line, mean snow thicknesses of 0.39 ± 0.06 m agreed within a centimeter with the mean of 0.38 m of W99, where W99 stated an RMS error of 0.09 m and an interannual variability of 0.06 m of their climatology. This excellent agreement demonstrates the validity and applicability of the W99 climatology in the multiyear ice zone, and suggests that there were no clear decadal snow thickness changes since its compilation in 1999. However, given the potential large interannual variability in snow accumulation and thickness and scarceness of accurate snow observations, long-term snow thickness change is still difficult to assess with certainty.

Figure 3a also shows that the 2Degree measurements east of the North Pole where somewhat thinner than the W99 results, 0.31 m compared with 0.36 m, respectively. This could be a result of the replacement of multiyear ice by predominantly first-year ice with thinner snow, which has taken place in this region since the W99 study (Haas et al., 2008; Kurtz & Farrell, 2011). However, the difference between snow on multiyear and first-year ice found here is much less than the 50% thinner snow on first-year ice commonly cited (Kurtz & Farrell, 2011). In addition, as comparison with the ArcticArc results suggests, differences can also be related to the smaller amount of data obtained during these ski expeditions potentially missing thicker snow on deformed ice when sampling less frequently. However, the differences between the snow on multiyear and first-year regions found here can also simply be due to interannual and regional variability. In contrast to our results in 2017, the ArcticArc data showed a strong latitudinal gradient of 0.02 m degree^{-1} from Greenland across the North Pole, with comparable site-to-site variability as in 2017 (Figure 3a; Gerland & Haas, 2011). Overall, in the region of the North Pole ArcticArc's snow was thinner by between 0.1 and 0.2 m than

observed in 2017 or by W99, again demonstrating the magnitude of possible interannual, regional, and methodological variability.

Our ice and snow thickness and snow salinity data can also be used to interpret observed radar backscatter in the study region. Our ice type classification is in general good agreement with the anticipated radar backscatter behavior. For example, the thickest site, nearest to Greenland, coincides with a region of very high backscatter indicative of strong ice deformation (Figure 1). Moreover, there is a drop in backscatter between the two northernmost sites associated with the transition from multiyear or second-year ice in the south to first-year ice in the north (Figure 1). Such transitions are important for the processing and interpretation of altimetry freeboard retrievals, and commonly, ice type masks provided by the EURMETSAT Ocean and Sea Ice Satellite Application Facility (OSISAF; Aaboe et al., 2016) are used. However, the map in Figure 1 shows that there is some disagreement between the locations of the ice type boundaries found by us and shown by OSISAF. This demonstrates the importance of ongoing validation of the OSISAF products and of an improved understanding of the effects of mixed ice types and product resolution that could have affected the OSISAF results.

We consider our measurements representative for a transect extending roughly from Ellesmere Island across the North Pole toward Siberia. However, some observation sites included in our analysis were partially offset zonally (Figure 1) and may therefore sample somewhat different ice regimes. Given additional interannual variability, this is difficult to assess with the 2017 and 2007 snow thickness data. However, the two sites sampled in 2017 in the northeast (Figure 1; triangles in Figure 3) clearly show some zonal differences, with mean and modal ice thicknesses both differing by up to 0.6 m compared to the main northwesterly transect. However, the radar backscatter map in Figure 1 also shows that the southeastern site was located in a strongly deformed region with high backscatter, and the northeastern site farther away from the shear zone than sites on the main profile at the same latitude, such that a direct comparison without consideration of ice flow lines remains difficult. Similarly, modal thicknesses of the two southern sites (Sites 1 and 2; Table S1) were only 2.4 m, well below the overall southward thickening gradient (Figure 3b). This could also be related to regional ice dynamics and the strong deformation in the East and replacement of older by younger ice before the ice bridge had stabilized.

5. Conclusions

We have presented results of rare in situ measurements of snow and ice thickness in the high Arctic Ocean. The measurements crossed the complete multiyear ice regime from the coast of Ellesmere Island across the Lincoln Sea toward the North Pole, into the first-year ice regime farther north. Snow thicknesses were highly variable from site to site, but overall mean thickness agreed well with the W99 climatology. This gives confidence in the use of the W99 climatology for altimetric sea ice freeboard retrievals in this region and suggests that long-term trends are difficult to observe. However, our measurements also indicated the possible magnitude of interannual variability and that differences between snow thickness on multiyear and first-year ice may be less than commonly assumed.

Our ice thickness results demonstrated that multiyear ice can still be more than 3 m thick but that its northern extent is limited. With this thickness, there is high probability that the ice will survive the summer melt season in the years to come. Overall results support other observations of continued thinning over the past decades, although changes are less clear in more recent years since 2011. Results are in line with other observations of Arctic sea ice shrinkage and implications for the future of Arctic climate, weather, and the ecosystem.

Although mean ice thicknesses are in reasonable agreement with extrapolated thickness trends computed by Lindsay and Schweiger (2015), our measurements may underestimate mean ice thickness due to undersampling of deformed ice and due to underestimation of deformed ice thickness by EM sounding. Therefore, we consider our modal thickness results more representative and indicative of changes in the thermodynamic forcing in the region.

Unfortunately, low-resolution satellite observations like those of the CryoSat, AltiKa, and SMOS missions cannot distinguish between mean and modal thicknesses. For those, the obtained information about mean snow thickness and its variability is most useful. However, our data will be most important for the validation of

higher-resolution remote sensing data like, for example, airborne OIB snow and ice thickness retrievals. Further analysis will be performed with regard to snow statistics (e.g., modal thicknesses) and ice and snow thickness covariability using the truly collocated data set. Our data can also be used for the evaluation and initialization of seasonal sea ice predictions.

Similar measurement campaigns should be repeated more routinely in the future to gather a more extensive and systematic data set of most accurate in situ snow and ice thickness for better evaluation of regional variations and interannual and long-term change. Our measurement protocol can easily be adopted by other groups, and as much data as possible should be obtained at each site. Therefore, the protocol for ski expeditions where normally only fewer measurements can be done should be carefully re-evaluated and adjusted. The gathered colocated, high-resolution snow and ice thickness data are also required for assessing the differences between first-year and multiyear ice with regard to their suitability as habitat for sea ice microorganisms and support of high algal biomasses. Our results confirm that even with a thick snow cover on average on multiyear ice, there are abundant locations with shallow or high hummocks with negligible snow cover where light levels underneath can be high enough to support algal growth (Lange et al., 2017). Our measurements have the potential to better assess the conditions of snow variability in support of deriving light level parameterizations and biophysical modeling.

Acknowledgments
Summaries of data gathered for this study are available in Table S1 of this manuscript. Raw data will be provided by the European Space Agency's (ESA) Earth Observation Campaigns Data web portal at https://earth.esa.int/web/guest/campaigns. CryoSat data were obtained from http://www.meereisportal.de and http://www.cpom.ucl.ac.uk/csopr/seaice.html. We are grateful for financial support by the European Space Agency's (ESA) CryoVEx campaigns, contract 4000120131/17/NL/FF/mg, Natural Sciences and Engineering Research Council (NSERC) and Canada Research Chair (CRC) programs, Alfred Wegener Institute for Polar and Marine Research (AWI), EU-funded ICE-ARC program, Environment and Climate Change Canada (ECCC), and NASA and ONR. We thank Andrew Platt, Jim Milne, and Chris Brown for their invaluable help with access to and working at CFS Alert, and staff at CFS Alert for their hospitality and great support. This project would not have been possible without the enthusiasm and professionalism of one of the most experienced ice pilots in the world, Captain Troy McKerral, and his crew from Kenn Borek Air, Calgary AB. They were backed by a Twin Otter operated by British Antarctic Survey.

References

Aaboe, S., Breivik, L.-A., Sorensen, A., Eastwood, S., & Lavergne, T. (2016). Global sea ice edge and type product user's manual-v1.3. Technical report SAF/OSI/CDOP2/MET-Norway/TEC/MA/205, EUMETSAT OSI SAF - Ocean and Sea Ice Satellite Application Facility.

Beckers, J. F., Haas, C., Elder, B., Hiemstra, C., Tilling, R., & Armitage, T. W. K. (2015). CryoVEx2014—In-situ measurements at MIZ/ONR and NORD (Greenland) ice camps, ESA Ground Team Report, ESA contract 4000110552/14/MP/vb, 46 pp.

Gerland, S., & Haas, C. (2011). Snow-depth observations by adventurers traveling on Arctic sea ice. *Annals of Glaciology*, *52*(57), 369–376.

Haas, C. (2017). Sea ice thickness distribution. In D. N. Thomas (Ed.), *Sea ice*, (3rd ed., pp. 42–64). Chichester, UK: John Wiley & Sons, Ltd.

Haas, C., Gerland, S., Eicken, H., & Miller, H. (1997). Comparison of sea-ice thickness measurements under summer and winter conditions in the Arctic using a small electromagnetic induction device. *Geophysics*, *62*(3), 749–757.

Haas, C., Hendricks, S., & Doble, M. (2006). Comparison of the sea ice thickness distribution in the Lincoln Sea and adjacent Arctic Ocean in 2004 and 2005. *Annals of Glaciology*, *44*, 247–252.

Haas, C., Hendricks, S., Eicken, H., & Herber, A. (2010). Synoptic airborne thickness surveys reveal state of Arctic sea ice cover. *Geophysical Research Letters*, *37*, L09501. https://doi.org/10.1029/2010GL042652

Haas, C., & Jochmann, P. (2003). Continuous EM and ULS thickness profiling in support of ice force measurements. In S. Loeset, B. Bonnemaire, & M. Bjerkas (Eds.), *Proceedings of the 17th International Conference on Port and Ocean Engineering under Arctic Conditions, POAC ´03, Trondheim, Norway*, (Vol. 2, pp. 849–856). Trondheim, Norway: Department of Civil and Transport Engineering, Norwegian University of Science and Technology NTNU.

Haas, C., Pfaffling, A., Hendricks, S., Rabenstein, L., Etienne, J.-L., & Rigor, I. (2008). Reduced ice thickness in Arctic transpolar drift favors rapid ice retreat. *Geophysical Research Letters*, *35*, L17501. https://doi.org/10.1029/2008GL034457

Hendricks, S., Ricker, R., & Helm, V. (2016). User guide—AWI CryoSat-2 sea ice thickness data product (v1.2). Retrieve from http://epic.awi.de/41242/

King, J., Howell, S., Derksen, C., Rutter, N., Toose, P., Beckers, J. F., … Richter-Menge, J. (2015). Evaluation of Operation IceBridge quick-look snow depth estimates on sea ice. *Geophysical Research Letters*, *42*, 9302–9310. https://doi.org/10.1002/2015GL066389

Kurtz, N. T., & Farrell, S. L. (2011). Large-scale surveys of snow depth on Arctic sea ice from Operation IceBridge. *Geophysical Research Letters*, *38*, L20505. https://doi.org/10.1029/2011GL049216

Kwok, R., & Cunningham, G. F. (2015). Variability of Arctic sea ice thickness and volume from CryoSat-2. *Philosophical Transactions of the Royal Society of London Series A*, *373*(2045). https://doi.org/10.1098/rsta.2014.0157, 20140157

Kwok, R., & Haas, C. (2015). Effects of radar sidelobes on snow depth retrievals from operation IceBridge. *Journal of Glaciology*, *61*(227), 576–584. https://doi.org/10.3189/2015JoG14J2292015

Lange, B. A., Flores, H., Michel, C., Beckers, J. F., Bublitz, A., Casey, J. A., … Haas, C. (2017). Pan-Arctic sea ice-algal chl a biomass and suitable habitat are largely underestimated for multi-year ice. *Global Change Biology*, *23*, 4581–4597. https://doi.org/10.1111/gcb.13742

Laxon, S. W., Giles, K. A., Ridout, A. L., Wingham, D. J., Willatt, R., Cullen, R., … Davidson, M. (2013). CryoSat-2 estimates of Arctic sea ice thickness and volume. *Geophysical Research Letters*, *40*, 732–737. https://doi.org/10.1002/grl.50193

Lindsay, R., Haas, C., Hendricks, S., Hunkeler, P., Kurtz, N., Paden, J., … Zhang, J. (2012). Seasonal forecasts of Arctic sea ice initialized with observations of ice thickness. *Geophysical Research Letters*, *39*, L21502. https://doi.org/10.1029/2012GL053576

Lindsay, R., & Schweiger, A. (2015). Arctic sea ice thickness loss determined using subsurface, aircraft, and satellite observations. *The Cryosphere*, *9*, 269–283. https://doi.org/10.5194/tc-9-269-2015

Meier, W. N., Hovelsrud, G. K., van Oort, B. E. H., Key, J. R., Kovacs, K. M., Michel, C., … Reist, J. D. (2014). Arctic sea ice in transformation: A review of recent observed changes and impacts on biology and human activity. *Reviews of Geophysics*, *52*, 185–217. https://doi.org/10.1002/2013RG000431

Notenboom, B., Daniels, A., & Hartley, M. (2017). Two degrees North Pole expedition, April 4–April 21 2017, Snow Measurement Data. Internal report (18 pp).

Perovich, D. K., & Richter-Menge, J. A. (2015). Regional variability in sea ice melt in a changing Arctic. *Philosophical Transactions of the Royal Society A*, *373*, 20140165. https://doi.org/10.1098/rsta.2014.0165

Renner, A. H. H., Gerland, S., Haas, C., Spreen, G., Beckers, J. F., Hansen, E., … Goodwin, H. (2014). Evidence of Arctic sea ice thinning from direct observations. *Geophysical Research Letters*, *41*, 5029–5036. https://doi.org/10.1002/2014GL060369

Richter-Menge, J. A., & Farrell, S. L. (2013). Arctic sea ice conditions in spring 2009–2013 prior to melt. *Geophysical Research Letters*, *40*, 5888–5893. https://doi.org/10.1002/2013GL058011

Stroeve, J., Blanchard-Wrigglesworth, E., Guemas, V., Howell, S., Massonnet, F., & Tietsche, S. (2015). Improving predictions of Arctic sea ice extent. *Eos*, *96*. https://doi.org/10.1029/2015EO031431

Sturm, M., Maslanik, J. A., Perovich, D. K., Stroeve, J. C., Richter Menge, J., Markus, T., … Tape, K. (2006). Snow depth and ice thickness measurements from the Beaufort and Chukchi seas collected during the AMSR-Ice03 campaign. *IEEE Transactions on Geoscience and Remote Sensing*, *44*(11), 3009–3020. https://doi.org/10.1109/TGRS.2006.878236

Tilling, R. L., Ridout, A., & Shepherd, A. (2016). Near-real-time Arctic sea ice thickness and volume from CryoSat-2. *The Cryosphere*, *10*(5), 2003–2012. https://doi.org/10.5194/tc-10-2003-2016

Verall, R. I. (2000). A guide to Arctic field trips. DREA TR 2000-094 Defence research establishment Atlantic, 156 pp.

Warren, S. G., Rigor, I. G., Untersteiner, N., Radionov, V. F., Bryazgin, N. N., Aleksandrov, Y. I., & Colony, R. (1999). Snow depth on Arctic sea ice. *Journal of Climate*, *12*(6), 1814–1829. https://doi.org/10.1175/1520-0442(1999)012%3C1814:SDOASI%3E2.0.CO;2

Willatt, R., & Haas, C. (2011). CryoVEx 2011 alert sea ice ground team report, Technical report, 88pp. Retrieve from https://earth.esa.int